ADVANCED BIOLOGY
www.advanced-bio.com

Coacervates Composed of Low-Molecular-Weight Compounds– Molecular Design, Stimuli Responsiveness, Confined Reaction

Sayuri L. Higashi and Masato Ikeda**

The discovery of coacervation within living cells through liquid–liquid phase separation has inspired scientists to investigate its fundamental principles and significance. Indeed, coacervates composed of low-molecular-weight compounds based on supramolecular strategy can offer valuable models for biomolecular condensates and useful tools. This mini-review highlights recent findings and advances in coacervates (artificial condensates), primarily composed of low-molecular-weight compounds, with focuses on their molecular design, stimuli responsiveness, and controlled reactions within or leading to the coacervates.

S. L. Higashi
Institute for Advanced Study
Gifu University
1-1 Yanagido, Gifu 501–1193, Japan
E-mail: higashi.sayuri.h0@f.gifu-u.ac.jp
S. L. Higashi, M. Ikeda
United Graduate School of Drug Discovery and Medical Information Sciences
Gifu University
1-1 Yanagido, Gifu 501–1193, Japan
E-mail: ikeda.masato.n3@f.gifu-u.ac.jp
S. L. Higashi, M. Ikeda
Center for One Medicine Innovative Translational Research (COMIT)
Institute for Advanced Study
Gifu University
1-1 Yanagido, Gifu 501–1193, Japan
M. Ikeda
Department of Chemistry and Biomolecular Science
Faculty of Engineering
Gifu University
1-1 Yanagido, Gifu 501–1193, Japan
M. Ikeda
Institute for Glyco-core Research (iGCORE)
Gifu University
1-1 Yanagido, Gifu 501–1193, Japan
M. Ikeda
Innovation Research Center for Quantum Medicine
Graduate School of Medicine
Gifu University
1-1 Yanagido, Gifu 501–1193, Japan

The ORCID identification number(s) for the author(s) of this article can be found under https://doi.org/10.1002/adbi.202400572

DOI: 10.1002/adbi.202400572

1. Introduction

Coacervates are micrometer-sized liquid compartments formed through phase separation under aqueous conditions. The term "coacervation," introduced by Bungenberg de Jong and Kruyt, derives from the Latin *acervus*, meaning aggregation, with the prefix "co" denoting togetherness.[1] Coacervation between oppositely charged polymers, such as charged proteins and polysaccharides, was first described in 1911.[2] In 2009, the discovery of membraneless organelles within living cells, resulting from in vivo liquid–liquid phase separation (LLPS),[3] brought renewed attention to the biological significance of coacervates. LLPS occurs when a homogeneous mixture spontaneously separates into two distinct liquid phases with differing component concentrations. It spurred active research into these phenomena and their properties.[4]

Over the past 15 years, substantial developments have been made in multidiscipline fields, including biology,[3,5] physiology,[6,7] particularly associated with diseases such as neurodegenerative disorders[8–11] and cancer,[12,13] as well as in materials science,[14,15] physics,[16] and the study of the origin of life.[17–19] We refer readers to recent reviews for detailed discussions.[3,5–19] In contrast, this mini-review highlights recent progress in coacervates, primarily composed of low-molecular-weight compounds (coacervators; in this review, we deal with compounds with their molecular weight up to ≈2500 as low-molecular-weight compounds) rather than polymers or proteins. Such coacervates are of increasing interest due to their potential applications in both biological systems and materials science. This review focuses specifically on coacervates (artificial condensates) composed of low-molecular-weight compounds, exploring their molecular design, stimuli-responsive behavior, and ability to control chemical reactions as illustrated in **Figure 1**.

2. Simple and Complex Coacervates

2.1. Molecular Design of Single Low-Molecular-Weight Building Blocks for Coacervates Formation–Simple Coacervates

In general, coacervates are divided into two typical types; simple coacervates and complex coacervates.[18] The simple coacervates are composed of single molecular components (e.g., sticker-spacer type molecules, amphiphilic molecules, and peptides; the chemical structures of 12 compounds capable of forming simple

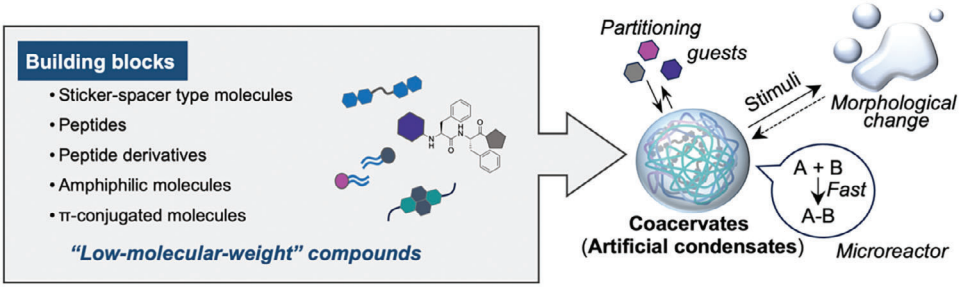

Figure 1. Coacervates (artificial condensates) are composed of low-molecular-weight compounds as building blocks and their applications.

coacervates are shown in **Figure 2**) whereas complex coacervates are composed of plural molecular components. The sticker-spacer model, where the sticker is a cohesive moiety and the spacer is a hydrophilic linear moiety, is one of the simplest to describe protein-mediated biomolecular condensate formation.[19] Biomolecular condensate has been known as an intracellular compartment called a membraneless organelle formed through LLPS. Biomolecular condensates are composed of various biomolecules (e.g., protein, nucleic acids), which spontaneously assemble into dense, liquid droplets that exist alongside the surrounding cytoplasm or nucleoplasm.[3,5] Successful developments in artificial condensates as simple coacervates have been made in the sticker-spacer model, particularly where two sticker sites are connected by a single linear spacer, which serves as the minimum structural requirement. A pioneering example by M. Abbas et al. demonstrated that introducing dipeptides at both ends of a spacer (Figure 2A-i) can lead to the formation of liquid droplets.[21,22] The amino acid compositions of the sticker dipeptides strongly influence the formation of coacervates as liquid droplets, with LL, LF, FL, and FF (**1**) sequences (F = phenylalanine, L = leucine) forming coacervates, while WF, FW, and WW (W = tryptophan) form aggregates most probably due to their excessive hydrophobicity. Beyond the properties of sticker dipeptides, the linear spacer's polarity also plays a crucial role in forming liquid-like coacervates. In detail, the authors disclosed the clear boundary between polar spacers with a zero or negative solvation-free energy, capable of forming coacervates, and apolar spacers with a positive solvation-free energy and limited aqueous solubility, resulting in aggregates. In a similar molecular design, Y. Bao et al. developed photo-responsive artificial condensates from a small molecule (**2**) comprising an oligoethylene glycol spacer bearing two hydrophobic pyrene groups instead of dipeptides (Figure 2A-ii).[23] In addition to this sticker-spacer model, Y. Tang et al. discovered that a simple dipeptide, QW (**3**; Q = glutamine, Figure 2A-iii), can form liquid droplets. This was achieved by carefully combining theoretical predictions using molecular dynamics simulations and experimental validation for selected dipeptides.[24] On the other hand, S. H. Hiew et al. reported that a longer bio-inspired peptide (Ac-GLYGGYGW-NH_2; G = glycine, Y = tyrosine), which is derived from the parent octapeptides (Ac-GLYGGYGX-NH_2; where X can be varied) from suckerin-19,[25] can also form coacervates.[26] This research emphasizes the critical importance of single amino acid residues in peptide sequences for coacervate formation. Deviations in the sequence may result in the formation of other self-assembled structures, such as fiber networks. This review primarily focuses on oligopeptides and their derivatives consisting of fewer than 10 amino acids. We direct readers to recent reviews for a more comprehensive discussion on natural and synthetic polypeptides and proteins.[27,28]

Further advancements in molecular engineering toward oligopeptides have proven effective for developing coacervates. C. Yuan et al. reported that a simple dipeptide derivative, Z-FF (**4**, Z = 4-benzyloxycarbonyl) (Figure 2A-iv), can form coacervates in a metastable state before the transition into fibrous structures (vide infra, Section 2.3.1).[29] In contrast, R. Kubota et al. discovered that a dipeptide (FF) derivative (**5**) with a *tert*-butyl ester (OtBu) at the C-terminus and a 4-phenyl-pyridinium cation at the N-terminus (Figure 2A-v) forms coacervates as liquid droplets.[30] Presumably, the bulky OtBu moiety of compound **5** plays an important role in the formation of liquid droplets as a stable state to avoid the transition to aggregates or fibrous structures. Recently, the same research group reported the formation of a unique sponge-like network within coacervates made from an in situ generated dipeptide (**6**) containing an oligo ethylene group instead of the 4-phenyl-pyridinium cation (Figure 2A-vi), revealing new insights into their structural dynamics.[31] Additionally, S. Cao et al. found that an FF-based molecule (**7**) with ester groups at its C-terminus (Figure 2A-vii) forms coacervates, which were utilized as active artificial organelles in both artificial cell models and living cells (discussed further in Section 2.4).[32] Besides oligopeptides, simple amino acids bearing aromatic groups, such as Fmoc-A, Fmoc-P, Fmoc-L,[29] and Fmoc-K[33] (Fmoc = 9-fluorenylmethoxycarbonyl, A = alanine, P = proline, K = lysine), can also form coacervates. Recently, S. Paul et al. elucidated the pathway complexity of pH-shift-induced self-assembly of Fmoc-L, with coacervates serving as key intermediates.[34] Most of the molecules above form coacervates as metastable states, a point further discussed later (Section 2.4).

Amphiphilic molecules have significant potential to form coacervates under specific aqueous conditions, particularly at higher concentrations.[35,36,37] A recent example involves the cationic single-chain surfactant, *N*-methylephedrinium bromide (DMEB, **8**, Figure 2B-i), which undergoes spontaneous phase separation to form coacervates in the presence of NaCl, $CaCl_2$, or $MgCl_2$.[38] Similarly, an amphiphilic ruthenium (II) tris(bipyridine) complex (**9**) bearing two hydrophobic alkyl chains (Figure 2B-ii) was shown to form coacervates in the presence of chaotropic counterions with larger radii and polarizability (e.g., NO_3^-, I^-), which reduce charge repulsion between cationic headgroups due to stronger binding affinity.[39] Likewise, most coacervates composed of ionic amphiphilic molecules can be obtained in the

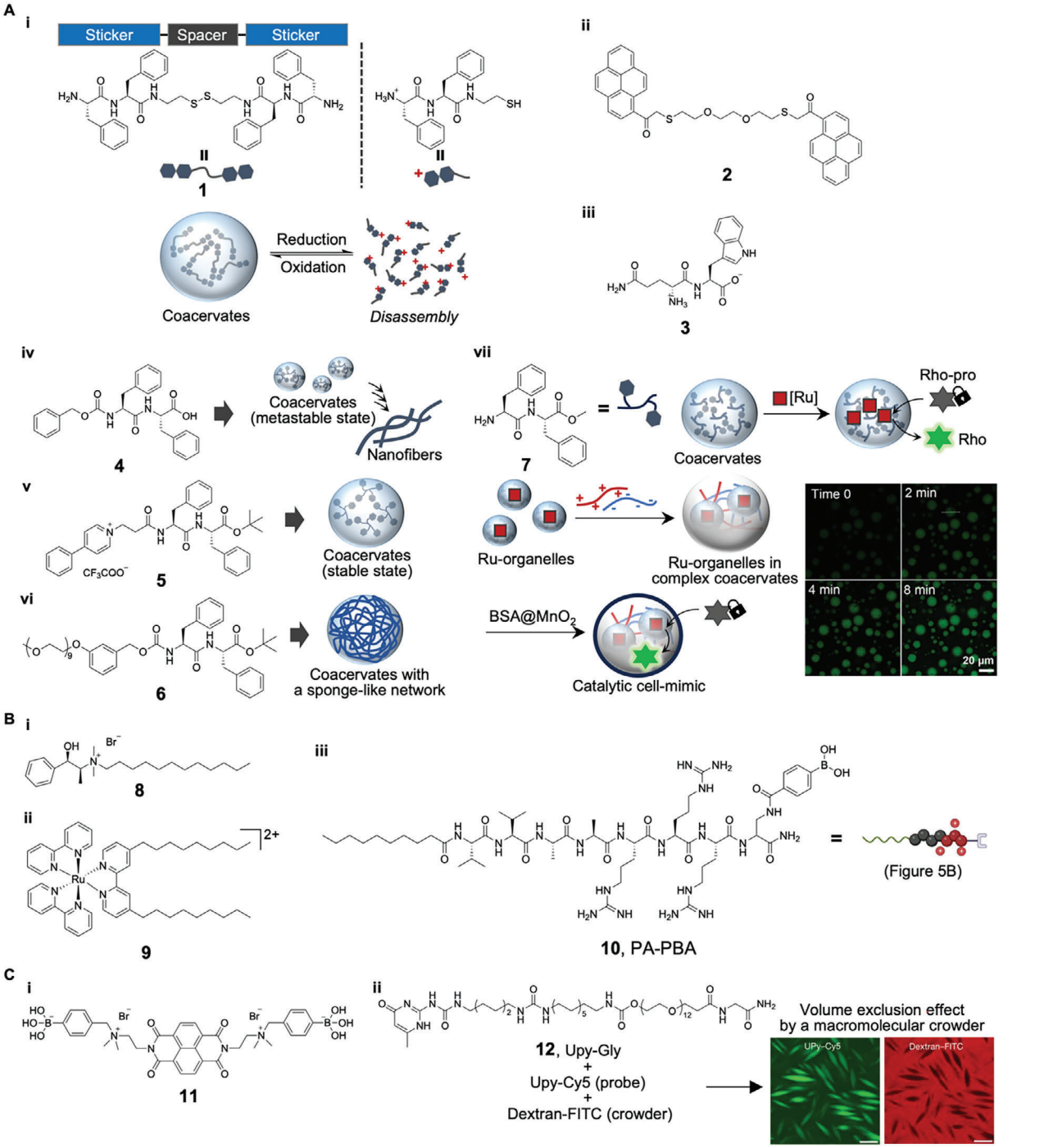

Figure 2. Molecular design for the construction of simple coacervates; **A** (i) Chemical structure of compound **1**[21] and schematic representation of redox-responsive coacervates composed of **1**. Chemical structures of (ii) compound **2**[23] and (iii) compound **3**,[24] both forming liquid droplets. (iv, v, vi) Chemical structures and schematic representations of coacervates composed of (iv) Z-FF (**4**),[29] (v) compound **5**,[30] and (vi) compound **6**.[31] vii) Chemical structure of compound **7** and schematic illustration of coacervates composed of **7**, entrapping a hydrophobic catalyst (Ru). Coacervates formed with Ru catalysts (Ru organelles) enabled the decaging of non-fluorescent Rho-pro, producing fluorescent rhodamine 110 (Rho). The scheme shows the construction of a catalytic cell mimic containing Ru organelles as artificial organelles. Confocal laser scanning microscopy (CLSM) images display the time-dependent formation of Rho (green fluorescence) by the cell mimics; scale bar: 20 μm. Reproduced under terms of the CC-BY license.[32] Copyright 2024, The Authors, published by Springer Nature. **B** Chemical structures of amphiphilic molecules forming coacervates: (i) compound **8**,[38] (ii) compound **9**,[39] and (iii) compound **10**.[40] Adapted with permission.[40] Copyright 2024 American Chemical Society. **C** (i) Chemical structure of compound **11**,[41] which forms metastable coacervates at alkaline pH. (ii) Chemical structure of compound **12**,[42] which forms anisotropic liquid droplets in the presence of a macromolecular crowder (dextran), accompanied by CLSM images. Reproduced under terms of the CC-BY license.[42] Copyright 2024, The Authors, published by Springer Nature.

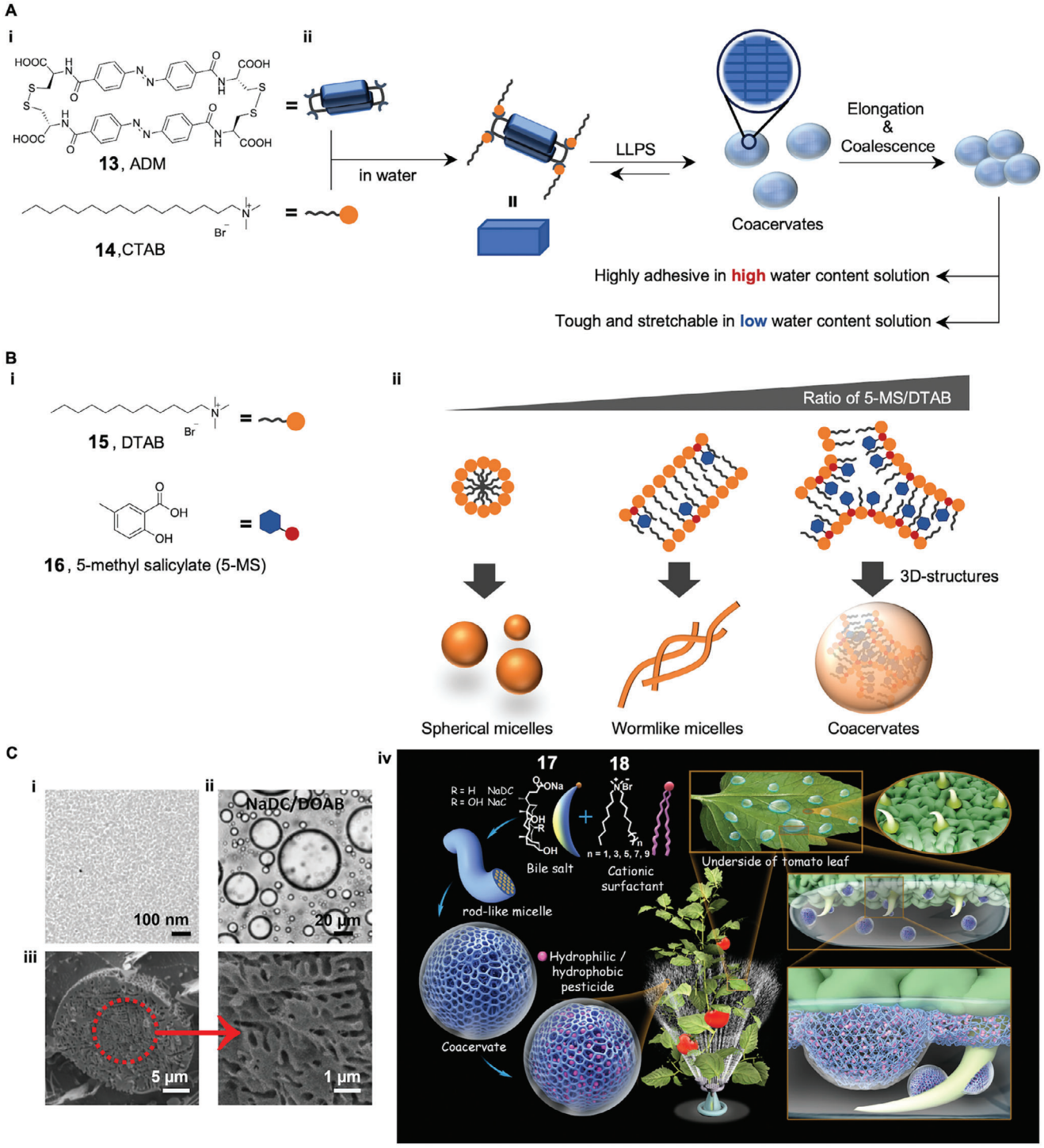

Figure 3. Molecular design for the construction of complex coacervates; **A** (i) Chemical structures of ADM (**13**) and CTAB (**14**),[43] and (ii) a scheme illustrating the process leading complex coacervates. **B** (i) Chemical structures of DTAB (**15**) and 5-MS (**16**),[44] and (ii) schematics representation for the formation of supramolecular architectures (spherical micelles, wormlike micelles, or complex coacervates) depending on the 5-MS/DTAB ratio. Adapted from.[44] Copyright 2023 Wiley VCH GmbH. **C** (i) Cryo-TEM image of rodlike micelles in a mixture of 20 mM NaDC (**17**, panel iv shows the chemical structure) with 20 mM of the oppositely charged surfactant (DOAB, **18**). (ii) Bright-field optical microscopic image and (iii) cryo-SEM image of coacervate microdroplets in a 30 mM NaDC/30 mM DOAB mixed solution. (iv) A scheme illustrating the strategy for constructing complex coacervates and controlling water-based pesticide spray on the superhydrophobic abaxial side of tomato leaves. Reproduced under terms of the CC-BY license.[45] Copyright 2023, The Authors, published by Wiley VCH GmbH.

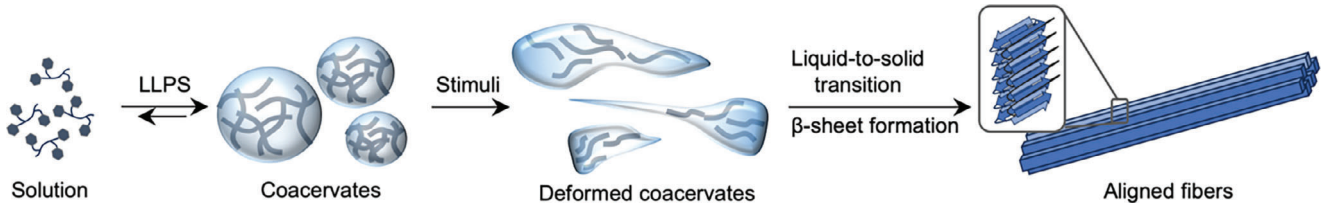

Figure 4. Transformations from coacervates to (aligned) fibrous structures induced by stimuli, i.e., pH, ionic strength, the Hofmeister effect, and shear flow.

presence of oppositely charged species; further examples related to complex coacervate formation are discussed in Section 2.2. In a different approach, S. Yu et al. reported that a peptide amphiphile bearing phenylboronic acid (PA-PBA, **10**) (Figure 2B-iii) could form coacervates in the presence of glucose (vide infra).[40] More recently, S. Patra et al. designed a naphthalene diimide (NDI)-derived molecule (**11**), which includes boronic acid and ammonium cation moieties, to form metastable droplets in a zwitterionic state at alkaline pH (Figure 2C-i).[41] Furthermore, a gradual transformation from droplets to fibrous structures over several days was manifested, which would be triggered by dominant π-π interactions between the π-conjugated NDI core. In most cases, coacervates appear as isotropic droplets; however, highly anisotropic liquid droplets were recently discovered in supramolecular polymers composed of ureidopyrimidinone glycine (Upy-Gly, **12**, Figure 2C-ii).[42] In the anisotropic liquid droplets, a highly ordered aqueous phase composed of the supramolecular polymers as high-aspect-ratio fibrils, like a liquid crystalline state, is generated. Interestingly, the shape of the anisotropic liquid droplet is not spherical but spindle-like as shown in CLSM images Figure 2C-ii.

2.2. Molecular Design of Ionic Low-Molecular-Weight Building Blocks to Give Coacervates by Complexation With Oppositely Charged Substances–Complex Coacervates

The low stability of the simple coacervates described above, mainly due to weak intermolecular forces (e.g., van der Waals, hydrogen bonding, π–π, and cation-π interactions), may present intrinsic challenges for low-molecular-weight compounds, which offer limited interaction sites at the molecular level. This can be a drawback when exploring their (bio) applications. Increasing intermolecular interactions is a reasonable strategy to enhance the stability of coacervates. Complex coacervations, fabricated via multiple ionic interactions in less polar environments formed by aggregated substances under aqueous conditions, may solve these stability issues.

Recently, J. Yu et al. reported that an anionic cyclic molecule (ADM, **13**), composed of azobenzene and cysteine for disulfide bond formation (**Figure 3A**), forms coacervates in the presence of a typical cationic amphiphile cetyltrimethylammonium bromide (CTAB, **14**).[43] The stoichiometric ratio between the anionic cyclic molecule (4–) and the cationic amphiphile (1+) is crucial, with a 1:4 molar ratio effectively neutralizing the charge. Notably, the study demonstrated that the coacervate-derived supramolecular materials were robust enough to exhibit macroscopic adhesive properties while remaining dynamic due to the disulfide bond's reducible nature, transforming into thiol groups. Similarly, Z. Liu et al. reported that a cationic surfactant, dodecyl trimethyl ammonium bromide (DTAB, **15**), formed coacervates when mixed with an excess amount of 5-methyl salicylate (5-MS, **16**), with a 30 mM concentration of 5-MS (against 20 mM DTAB) (Figure 3B).[44] Remarkably, these coacervates exhibited ice growth inhibition properties, which were utilized for effective cryopreservation of human mesenchymal stem cells. A systematic investigation of sodium (doxy)cholates, or Na(D)C, and ammonium cations revealed the formation of coacervates when Na(D)C (e.g., **17**) were mixed with alkylammonium halides bearing two alkyl chains (e.g., **18**) at higher concentrations (Figure 3C).[45] The coacervates demonstrated efficient encapsulation of various solutes, including pesticides, and showed strong adhesion to surfaces with nano- and micro-morphologies, facilitating effective pesticide deposition on tomato leaves (Figure 3C-iv). As an example of converting cationic amphiphiles to anionic ones, L. Zhou et al. reported the formation of coacervates by mixing decanoic acid with dopamine. The optimization of coacervate formation was explored in terms of concentration, molar ratio, pH, and temperature.[46]

Polyoxometalates (POMs) are an attractive class of polyanionic materials with well-defined topologies and useful properties. Mixing a cationic amino acid, arginine, with $K_8[\alpha\text{-}SiW_{11}O_{39}]$ (SiW_{11}), a representative POM, formed coacervate.[47] Additionally, cationic tripeptides (GHK, GFK, GVK; H = histidine) also formed coacervates when mixed with SiW_{11}.[48]

Other than those above, coating coacervates with lipid membranes,[49] polymers,[40,50–52] or proteins[53] is a promising strategy to enhance their stability further, though this may compromise their dynamic characteristics.

2.3. Stimuli Responsiveness of Coacervates

2.3.1. Transformation From Metastable Coacervates Into More Thermodynamically Stable Structures

Similar to the behavior of biomolecular condensates, particularly those related to disease-associated proteins,[4,8] coacervates (artificial condensates) can occasionally transform fibrous structures. This transformation is often driven by common aqueous conditions such as pH, ionic strength, and the Hofmeister effect (**Figure 4**). These are closely linked to forming metastable coacervates that eventually evolve into fibrous structures.[34,41] In this context, metastable coacervates refer to intermediate states that are not fully stable but can exist long enough to undergo structural transitions, such as phase separation into more thermodynamically stable forms. Notably, shear-mediated transformations from coacervates to fibrous structures have

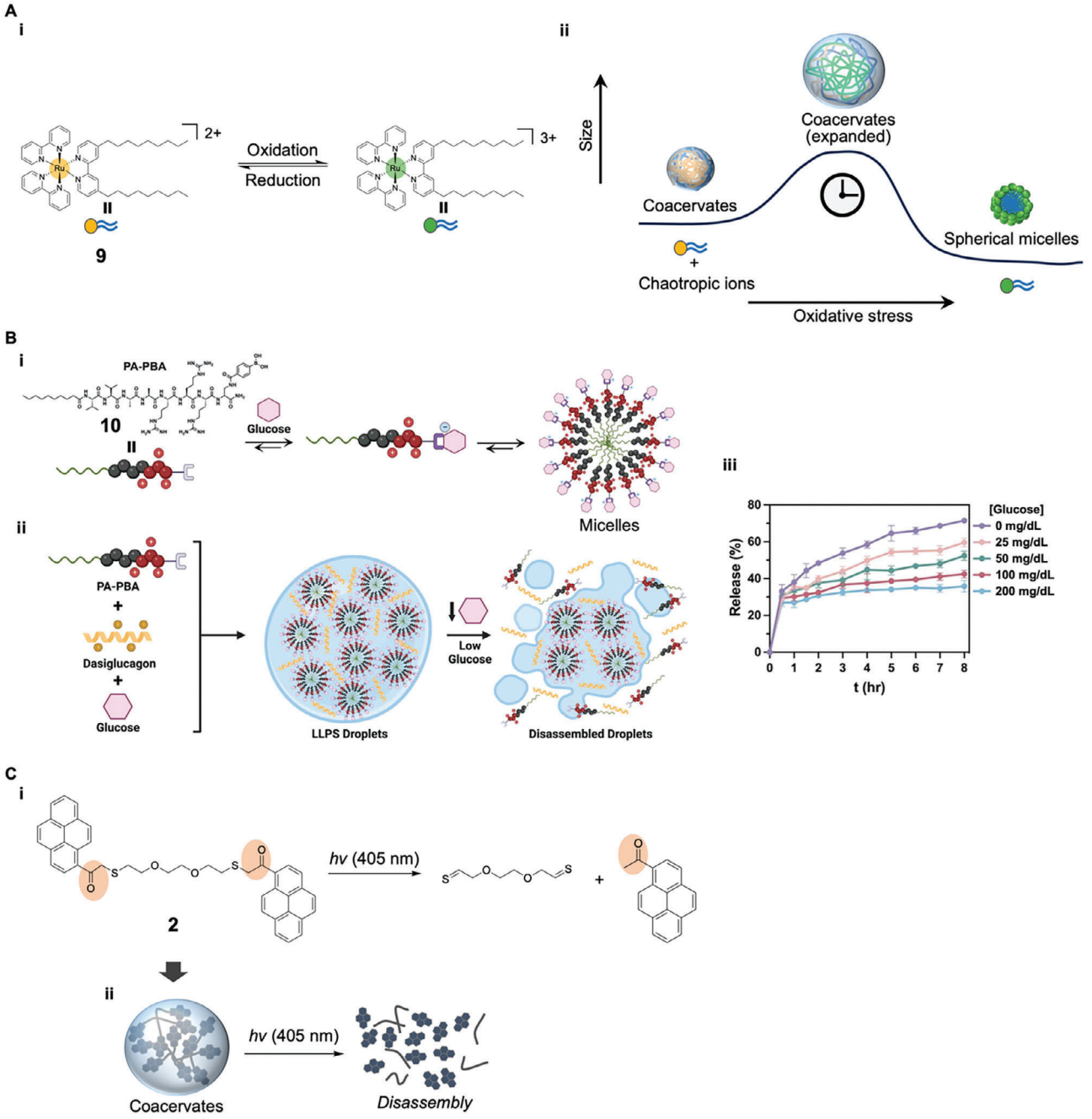

Figure 5. Disassembly of coacervates in response to stimuli; **A** (i) Chemical structures of compound **9**[39] in different redox states, and (ii) a schematic diagram showing the oxidation-triggered coacervate–to–expanded coacervate–to–micelle transition. Adapted with permission.[39] Copyright 2023 Wiley VCH GmbH. **B** (i) Complex formation of PA-PBA (**10**)[40] with glucose, leading to micelle formation, (ii) schematic representation of hypoglycemia-triggered disassembly of coacervates (LLPS droplets) composed of **10**-glucose micelles and dasiglucagon, and (iii) hypoglycemia-dependent dasiglucagon release (%) profiles. Adapted with permission.[40] Copyright 2024 American Chemical Society. **C** (i) Photo-induced Norrish type II reaction of compound **2**,[23] and (ii) schematic representations of the photo-responsive disassembly of coacervates formed by compound **2**.

been observed, emphasizing the significant role of physical and chemical factors in facilitating these transitions.[54] Importantly, the role of shear stress and LLPS in forming spider silk from polypeptides have also been studied, highlighting the relevance of these factors in biological contexts.[55]

2.3.2. Controlled Transformation or Disassembly of Coacervates in Response to Stimuli

Controlled transformation or disassembly of coacervates is advantageous for various (bio) applications, such as the

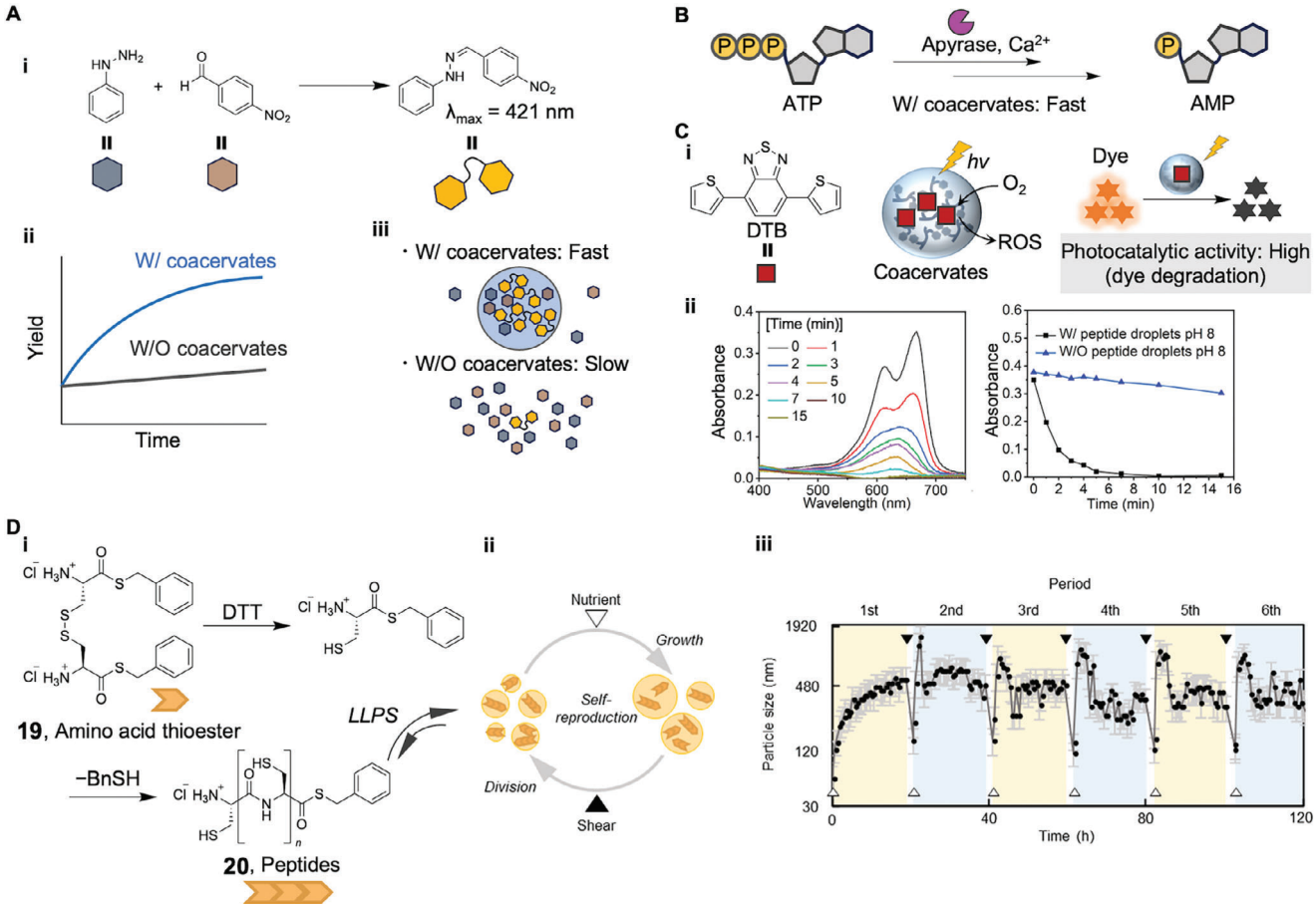

Figure 6. Controlled reactions in coacervates and to form coacervates; **A** (i) Chemical reaction scheme of hydrazone formation between phenylhydrazine and *p*-nitrobenzaldehyde. (ii) Time-dependent hydrazone formation with (gray) and without (blue) coacervates, and (iii) schematic illustrating the compartmentalization effect of coacervates on hydrazone formation (coacervates enhance the hydrazone production through substrate compartmentalization).[21] **B** Enhanced ATP hydrolysis by apyrase in the presence of amphiphile(**8**)-based coacervates.[38] **C** (i) Chemical structure of DTB (photocatalyst) and schematic representations of dipeptide(**7**)-based photocatalytic microreactor containing DTB (DTB-microreactor) for methylene blue dye degradation.[32] (ii) (left) Absorption spectral changes during the photocatalytic degradation of methylene blue by the DTB-microreactor and (right) the corresponding time-dependent absorbance changes with (W/) and without (W/O) the DTB-microreactor. Reproduced under the terms of the CC-BY license.[32] Copyright 2024, The Authors, published by Springer Nature. **D** Autocatalytic reaction and molecular assembly starting from an amino acid thioester (**19**) leading to self-reproducing coacervates. (i) Chemical reactions producing oligopeptides (**20**) for coacervate formation, (ii) the growth–division cycle of self-reproducing coacervates, and (iii) the cycle of coacervates growth with the addition of amino acid thioester (**19**; nutrient, white triangle) and coacervate division in response to an applied stimulus (shear, black triangle). Reproduced under the terms of the CC-BY license.[58] Copyright 2021, The Authors, published by Springer Nature.

active release of encapsulated substances. For example, pH-responsiveness is commonly implemented in coacervates constructed from molecules bearing ionizable groups, such as amino groups.[21,32] In contrast, reduction responsiveness has been achieved more purposely by introducing disulfide groups into the spacer of sticker-spacer model molecules, such as the peptide derivative (**1**) mentioned earlier (Figure 2A-i).[21] Additionally, controlling the redox state of the metal center in the amphiphile (**9**) enabled the manipulation of coacervate structures (**Figure** 5A-i).[39] Specifically, oxidation of the metal center (from Ru^{II} to Ru^{III}) induced non-monotonic morphological changes, i.e., the coacervate expansion, contraction, and eventually transformation into small micelles with the formation of hydrophobic core fabricated by alkyl chains (Figure 5A-ii). Host-guest interactions are also useful for incorporating more specific chemical stimuli responsiveness. For instance, coacervates composed of PA-PBA (**10**), which bears boronic acids (Figure 5B), were sensitive to glucose concentration. This enabled the controlled release of encapsulated biologics, such as dasiglucagon (a therapeutic hormone analog), in response to lowered glucose levels (hypoglycemia) (Figure 5B-ii,iii).[40]

Photo-responsiveness allows for spatiotemporally controlled transformation or disassembly of coacervates. For example, a Norrish carbonyl group introduced into compound **2** (Figure 5C-i) enabled photocleavage of the linker between the sticker and the spacer via the Norrish type II reaction, which led to the disassembly of the coacervate (Figure 5C-ii).[23] Since coacervates can encapsulate a variety of proteins and facilitate intracellular protein delivery, photo-responsive disassembly (induced by 405 nm light, but not by 488, 456, or 440 nm) resulted

in the intracellular, cytosolic distribution of the encapsulated payloads. Among the different stimuli-responsive systems discussed, photo- and redox-responsive coacervates could offer the advantage of selective control over disassembly. Each approach has its trade-offs in terms of versatility and reliability in its molecular design.

2.4. Controlled Reactions in Coacervates

Compartmentalization within the microenvironments of coacervates enables the encapsulation of client molecules, including reactants and (bio) catalysts, which increases the local concentrations and modulates the microscale conditions around the reactants. This is expected to control the rate of target reactions effectively.[56,57] For example, the hydrazone formation reaction between an aldehyde and hydrazine is accelerated in the presence of peptide(**1**)-based coacervates (**Figure 6A**).[21] Similarly, the rate enhancement of ATP hydrolysis by apyrase is observed in amphiphile(**8**)-based coacervates (Figure 6B).[38] A more specific example includes the enhanced activity of a hydrophobic photocatalyst (DTB: 4,7-di(2-thienyl)-2,1,3-benzothiadiazole) within peptide(**7**)-based coacervates (Figure 6C).[32] DTB was efficiently sequestered within the peptide-based coacervates and showed higher performance of dye degradation by ROS (reactive oxygen species) generated upon light irradiation within the coacervates, compared to free DTB without the coacervates. This is a representative example that coacervates provide a suitable microenvironment that maintains the activity of a water-insoluble catalyst in the aqueous media. Additionally, encapsulating a hydrophobic ruthenium (II) catalyst, chloro(pentamethylcyclopentadienyl)(cyclooctadiene)ruthenium(II) [CPRu(cod)Cl], inside these coacervates has allowed for the development of artificial organelles that function as even inside living cells (Figure 2A-vii). In another example, M. Matsuo et al. reported the spontaneous formation of coacervates during oligopeptide synthesis, starting from an initial amino acid thioester (**19**) (Figure 6D).[58] Interestingly, an autocatalytic process producing oligopeptides (**20**), primarily di-, tri-, and tetrapeptides, was revealed, allowing for self-reproduction via a growth–division cycle through the periodic addition of thioester monomers (Figure 6D-iii). This system supports the research direction of the origins-of-life theories, particularly the coacervate or droplet world hypothesis.

3. Conclusion

This review highlights recent research on the molecular design for coacervate development, incorporating stimuli responsiveness and controlled reactions within coacervates. The revisited supramolecular strategy, employing a bottom-up approach to create new coacervates, offers valuable models for biomolecular condensates and useful tools. However, the availability of low-molecular-weight compounds remains limited, and their applications are still in the early stages of exploration. Thus, academics and industrial scientists need to conduct further research on this promising class of materials to expand the scope of future applications. The stimuli-responsive coacervates discussed in this review hold significant potential for applications in areas such as controlled drug delivery, where pH- and redox-responsive systems could allow for targeted release in different physiological environments. Additionally, the enhanced catalytic activity observed in peptide-based coacervates suggests their utility in industrial catalysis and environmental remediation.

Acknowledgements

This work was supported in part by MEXT/JSPS KAKENHI (23K19212 and 24H01126 to S.L.H., 23H01815 to M.I.), Tokai Pathways to Global Excellence (T-GEx), part of MEXT Strategic Professional Development Program for Young Researchers (S.L.H.), and Toyota Riken Research Grants. The authors thank Enago (www.enago.jp) for the English language review.

Conflict of Interest

The authors declare no conflict of interest.

Data Availability Statement

The data that support the findings of this study are available from the corresponding author upon reasonable request.

Keywords

coacervate, condensate, liquid–liquid phase separation, self-assembly, stimuli responsiveness, supramolecular materials

Received: September 25, 2024
Revised: January 9, 2025
Published online: February 12, 2025

[1] H. G. Bungenberg de Jong, H. R. Kruyt, *Proc. Koninkl. Med. Akad. Wetershap.* **1929**, *32*, 849.
[2] F. W. Z. Tiebackx, *Chem. Ind. Kolloide* **1911**, *8*, 198.
[3] C. P. Brangwynne, C. R. Eckmann, D. S. Courson, A. Rybarska, C. Hoege, J. Gharakhani, F. Jülicher, A. A. Hyman, *Science* **2009**, *324*, 1729.
[4] Y. Shin, C. P. Brangwynne, *Science* **2017**, *357*, eaaf4382.
[5] S. F. Banani, H. O. Lee, A. A. Hyman, M. K. Rosen, *Nat. Rev. Mol. Cell Biol.* **2017**, *18*, 285.
[6] C. Wei, M. Li, X. Li, J. Lyu, X. Zhu, *Adv. Biology* **2022**, *6*, 2200006.
[7] S. Boeynaems, S. Chong, J. Gsponer, L. Holt, D. Milovanovic, D. M. Mitrea, O. Mueller-Cajar, B. Portz, J. F. Reilly, C. D. Reinkemeier, B. R. Sabari, S. Sanulli, J. Shorter, E. Sontag, L. Strader, J. Stachowiak, S. C. Weber, M. White, H. Zhang, M. Zweckstetter, S. Elbaum-Garfinkle, R. Kriwacki, *J. Mol. Biol.* **2023**, *435*, 167971.
[8] B. Wolozin, P. Ivanov, *Nat. Rev. Neurosci.* **2019**, *20*, 649.
[9] S. Ray, N. Singh, R. Kumar, K. Patel, S. Pandey, D. Datta, J. Mahato, R. Panigrahi, A. Navalkar, S. Mehra, L. Gadhe, D. Chatterjee, A. S. Sawner, S. Maiti, S. Bhatia, J. A. Gerez, A. Chowdhury, A. Kumar, R. Padinhateeri, R. Riek, G. Krishnamoorthy, S. K. Maji, *Nat. Chem.* **2020**, *12*, 705.
[10] A. Agarwal, S. K. Rai, A. Avni, S. Mukhopadhyay, *Proc. Natl. Acad. Sci. U.S.A.* **2021**, *118*, 2100968118.
[11] S. Mukherjee, M. Poudyal, K. Dave, P. Kadu, S. K. Maji, *Chem. Soc. Rev.* **2024**, *53*, 4976.

[12] J. Ren, Z. Zhang, Z. Zong, L. Zhang, F. Zhou, *Adv. Sci.* **2022**, *9*, 2202855.
[13] S. Spannl, M. Tereshchenko, G. J. Mastromarco, S. J. Ihn, H. O. Lee, *Traffic* **2019**, *20*, 890.
[14] A. Huang, L. Su, *Acc. Mater. Res.* **2023**, *4*, 729.
[15] Y. Song, *Biomater. Sci.* **2024**, *12*, 1943.
[16] V. Marx, *Nat. Methods* **2020**, *17*, 567.
[17] B. Ghosh, R. Bose, T.-Y. D. Tang, *Curr. Opin. Colloid Interface Sci.* **2021**, *52*, 101415.
[18] Z. Lin, T. Beneyton, J. C. Baret, N. Martin, *Small Methods* **2023**, *7*, 2300496.
[19] S. Kuila, J. Nanda, *ChemSystemsChem* **2024**, *6*, 202400022.
[20] E. W. Martin, A. S. Holehouse, I. Peran, M. Farag, J. J. Incicco, A. Bremer, C. R. Grace, A. Soranno, R. V. Pappu, T. Mittag, *Science* **2020**, *367*, 694.
[21] M. Abbas, W. P. Lipiński, K. K. Nakashima, W. T. S. Huck, E. Spruijt, *Nat. Chem.* **2021**, *13*, 1046.
[22] M. Abbas, J. O. Law, S. N. Grellscheid, W. T. S. Huck, E. Spruijt, *Adv. Mater.* **2022**, *34*, 2202913.
[23] Y. Bao, H. Chen, Z. Xu, J. Gao, L. Jiang, J. Xia, *Angew. Chem., Int. Ed.* **2023**, *62*, 202307045.
[24] Y. Tang, S. Bera, Y. Yao, J. Zeng, Z. Lao, X. Dong, E. Gazit, G. Wei, *Cell Rep. Phys. Sci.* **2021**, *2*, 100579.
[25] S. H. Hiew, P. A. Guerette, O. J. Zvarec, M. Phillips, F. Zhou, H. Su, K. Pervushin, B. P. Orner, A. Miserez, *Acta Biomater.* **2016**, *46*, 41.
[26] S. H. Hiew, Y. Lu, H. Han, R. A. Gonçalves, S. R. Alfarano, R. Mezzenga, A. N. Parikh, Y. Mu, A. Miserez, *J. Am. Chem. Soc.* **2023**, *145*, 3382.
[27] M. Abbas, W. P. Lipiński, J. Wang, E. Spruijt, *Chem. Soc. Rev.* **2021**, *50*, 3690.
[28] A. Sathyavageeswaran, J. Bonesso Sabadini, S. L. Perry, *Acc. Chem. Res.* **2024**, *57*, 386.
[29] C. Yuan, A. Levin, W. Chen, R. Xing, Q. Zou, T. W. Herling, P. K. Challa, T. P. J. Knowles, X. Yan, *Angew. Chem., Int. Ed.* **2019**, *58*, 18116.
[30] R. Kubota, S. Torigoe, I. Hamachi, *J. Am. Chem. Soc.* **2022**, *144*, 15155.
[31] R. Kubota, T. Hiroi, Y. Ikuta, Y. Liu, I. Hamachi, *J. Am. Chem. Soc.* **2023**, *145*, 18316.
[32] S. Cao, T. Ivanov, J. Heuer, C. T. J. Ferguson, K. Landfester, L. C. Silva, *Nat. Commun.* **2024**, *15*, 39.
[33] N. Narang, T. Sato, *Polym. J.* **2021**, *53*, 1413.
[34] S. Paul, K. Gayen, P. G. Cantavella, B. Escuder, N. Singh, *Angew. Chem., Int. Ed.* **2024**, *63*, 202406220.
[35] W. Zhao, Y. Wang, *Adv. Colloid Interface Sci.* **2017**, *239*, 199.
[36] N. Martin, J. P. Douliez, *ChemSystemsChem* **2021**, *3*, 2100024.
[37] X. Xiao, L. Jia, J. Huang, Y. Lin, Y. Qiao, *Chem. Asian J.* **2022**, *17*, 202200938.
[38] L. Zhou, Y. Fan, Z. Liu, L. Chen, E. Spruijt, Y. Wang, *CCS Chem* **2021**, *3*, 358.
[39] Y. Yan, W. Mu, H. Li, C. Song, Y. Qiao, Y. Lin, *Adv. Mater.* **2023**, *35*, 2210700.
[40] S. Yu, W. Chen, G. Liu, B. Flores, E. L. DeWolf, B. Fan, Y. Xiang, M. J. Webber, *J. Am. Chem. Soc.* **2024**, *146*, 7498.
[41] S. Patra, S. Chandrabhas, S. Dhiman, S. J. George, *J. Am. Chem. Soc.* **2024**, *146*, 12577.
[42] H. Fu, J. Huang, J. J. B. vanderTol, L. Su, Y. Wang, S. Dey, P. Zijlstra, G. Fytas, G. Vantomme, P. Y. W. Dankers, E. W. Meijer, *Nature* **2024**, *626*, 1011.
[43] J. Yu, D. Qi, E. Mäkilä, L. Lassila, A. C. Papageorgiou, M. Peurla, J. M. Rosenholm, Z. Zhao, P. Vallittu, S. Jalkanen, C. Jia, J. Li, *Angew. Chem., Int. Ed.* **2022**, *61*, 202204611.
[44] Z. Liu, H. Cao, Y. Fan, Y. Wang, J. Wang, *Angew. Chem., Int. Ed.* **2023**, *62*, 202311047.
[45] L. Zhang, J. Wang, Y. Fan, Y. Wang, *Adv. Sci.* **2023**, *10*, 2300270.
[46] L. Zhou, J. J. Koh, J. Wu, X. Fan, H. Chen, X. Hou, L. Jiang, X. Lu, Z. Li, C. He, *Bioconjug. Chem.* **2022**, *33*, 444.
[47] X. Liu, X. Xie, Z. Du, B. Li, L. Wu, W. Li, *Soft Matter* **2019**, *15*, 9178.
[48] X. Li, T. Zheng, X. Liu, Z. Du, X. Xie, B. Li, L. Wu, W. Li, *Langmuir* **2019**, *35*, 4995.
[49] X. Lv, J. Liu, P. Song, L. Zhao, Y. Lin, *ChemSystemsChem* **2024**, *6*, 202300040.
[50] Y. Ji, Y. Lin, Y. Qiao, *J. Am. Chem. Soc.* **2023**, *145*, 12576.
[51] Y. Ji, Y. Qiao, *Commun. Chem.* **2024**, *7*, 122.
[52] M. Naz, L. Zhang, C. Chen, S. Yang, H. Dou, S. Man, J. Li, *Commun. Chem.* **2024**, *7*, 79.
[53] X. Wang, X. Liu, X. Huang, *Adv. Mater.* **2020**, *32*, 2001436.
[54] Y. Shen, F. S. Ruggeri, D. Vigolo, A. Kamada, S. Qamar, A. Levin, C. Iserman, S. Alberti, P. St George-Hyslop, T. P. J. Knowles, *Nat. Nanotechnol.* **2020**, *15*, 841.
[55] J. Chen, A. Tsuchida, A. D. Malay, K. Tsuchiya, H. Masunaga, Y. Tsuji, M. Kuzumoto, K. Urayama, H. Shintaku, K. Numata, *Nat. Commun.* **2024**, *15*, 527.
[56] I. B. A. Smokers, B. S. Visser, A. D. Slootbeek, W. T. S. Huck, E. Spruijt, *Acc. Chem. Res.* **2024**, *57*, 1885.
[57] S. Lim, D. S. Clark, *Trends Biotechnol.* **2024**, *42*, 496.
[58] M. Matsuo, K. Kurihara, *Nat. Commun.* **2021**, *12*, 5487.

Sayuri L. Higashi received her Ph.D. in 2021 from Gifu University (Japan) under the supervision of Prof. Masato Ikeda. In 2021–2023, she carried out postdoctoral research at the Institute for Physiological Chemistry and Patho-biochemistry, University of Münster (Germany, PI: Prof. Seraphine V. Wegner). In 2023, she became a project assistant professor at Gifu University. Her research interest is to develop functional supramolecular systems as life-like materials.

Masato Ikeda received his Ph.D. in 2002 from Kyushu University (Japan). In 2003–2004, he carried out postdoctoral research at University of Strasbourg (France). In 2004–2006, he joined JST, ERATO Project as a researcher. In 2006, he became an assistant professor at Kyushu University. In 2007, he moved to Kyoto University (Japan) as an assistant professor. In 2012, he moved to Gifu University as an associate professor and was promoted to full professor in 2017. His research interest is to develop functional supramolecular materials and molecular hybrids for bio-applications.